



Universal Scaling and Critical Exponents of the Anisotropic Quantum Rabi Model

Maoxin Liu,¹ Stefano Chesi,^{1,*} Zu-Jian Ying,^{1,†} Xiaosong Chen,^{2,3} Hong-Gang Luo,^{4,1,‡} and Hai-Qing Lin¹

¹Beijing Computational Science Research Center, Beijing 100193, China

²Institute of Theoretical Physics, Chinese Academy of Sciences, P.O. Box 2735, Beijing 100190, China

³School of Physical Sciences, University of Chinese Academy of Sciences, Beijing 100049, China

⁴Center for Interdisciplinary Studies and Key Laboratory for Magnetism

and Magnetic Materials of the MoE, Lanzhou University, Lanzhou 730000, China

(Received 21 February 2017; revised manuscript received 21 July 2017; published 28 November 2017)

We investigate the quantum phase transition of the anisotropic quantum Rabi model, in which the rotating and counterrotating terms are allowed to have different coupling strengths. The model interpolates between two known limits with distinct universal properties. Through a combination of analytic and numerical approaches, we extract the phase diagram, scaling functions, and critical exponents, which determine the universality class at finite anisotropy (identical to the isotropic limit). We also reveal other interesting features, including a superradiance-induced freezing of the effective mass and discontinuous scaling functions in the Jaynes-Cummings limit. Our findings are extended to the few-body quantum phase transitions with $N > 1$ spins, where we expose the same effective parameters, scaling properties, and phase diagram. Thus, a stronger form of universality is established, valid from $N = 1$ up to the thermodynamic limit.

DOI: [10.1103/PhysRevLett.119.220601](https://doi.org/10.1103/PhysRevLett.119.220601)

Introduction.—While critical phenomena are traditionally associated with collective behavior in the thermodynamic limit, quantum phase transitions (QPTs) in systems with few degrees of freedom were recently brought to prominence [1,2]. As it turns out, the topic is of great relevance for ongoing efforts on enhancing and engineering light-matter interactions. By achieving the strong [3,4], ultrastrong [5–11], and even deep strong coupling regimes [12–16], atomic and solid-state resonances are able to induce profound modifications of the photon fields they interact with. The quantum Rabi model (QRM), describing a two-level system coupled to a single electromagnetic mode, represents the simplest realization of such light-matter interactions. Thus, it has served as a paradigmatic example to explore this kind of strong coupling phenomena and has received renewed attention in recent years [1,17–26].

Remarkably, an analytic solution of the QRM was found only recently and has also motivated proposing a novel operational criterion of integrability [18]. More directly related to the present study are several recent analyses on the dependence of QRM ground-state properties on the coupling strength [1,22,24]. Among these, Ref. [24] introduced a variational ansatz based on the polaron and antipolaron concepts and demonstrated a phase diagram where the quadpolaron (bipolaron) dominates in the weak (strong) coupling regime. The crossover becomes sharper by reducing the bosonic frequency [22,24], and it was later proved that this behavior indeed reflects the existence of a true QPT, whose static and dynamical properties were studied in detail [1,26]. The same type of QPT occurs in the Jaynes-Cummings (JC) model [2] and in the anisotropic QRM [27,28], where the JC and QRM become special cases. The asymmetry between rotating and counterrotating terms is

relevant for a variety of systems, including quantum wells with spin-orbit coupling [29,30] (possibly emulated by fermionic gases) and circuit QED, where strong interactions were already achieved [3,4,6,11,14–17]. In the latter case, the anisotropic QRM is naturally realized [27,31,32] and is experimentally relevant [17,32]. Such a model can also be implemented with trapped ions [26,33], and cavity QED [34] might allow for alternative realizations.

In the present study, we approach the QPT from the point of view of universality classes, motivated by the different types of broken symmetry phase of the JC and QRM critical points [1,2]. The problem has general interest, since the existence of universality classes can be understood from a coarse-grained description, where microscopic features become irrelevant. However, this argument is not directly applicable to few-body systems, so it is unclear if established knowledge is still valid. On the other hand, the remarkable similarity between the behavior found in Refs. [1,2,27,28] and the Dicke model, e.g., the precise form of the phase diagram [31], suggests that few-body QPTs could be understood through a direct equivalence to regular QPTs.

Indeed, by developing the low-energy theory describing critical scaling, we find that this is the case. Not only do we establish that the $\lambda \neq 0$ QPTs belong to a well-defined universality class, but we extend our treatment to $N > 1$ spins, thus bridging the gap between the few-body and thermodynamic QPTs. The identical behavior is valid for any finite N , includes nonuniversal features, and reconciles a series of previously disconnected results [1,2,26–28,31]. Our treatment further reveals the unusual renormalization of the $\lambda \neq 0$ effective mass and the singular character of the JC limit, where successive discontinuities exist across the whole critical regime.

Model.—In terms of the $x = (a^\dagger + a)/\sqrt{2}$ and $p = i(a^\dagger - a)/\sqrt{2}$ quadratures (with a^\dagger a bosonic creation operator), the Dicke model with anisotropy [31] reads ($\hbar = 1$)

$$\frac{H}{N\Omega} = \frac{p^2 + x^2}{2\eta} + \frac{J_x}{N} + \frac{\tilde{g}}{N} \left[\frac{1+\lambda}{\sqrt{2\eta}} J_z x + \frac{1-\lambda}{\sqrt{2\eta}} J_y p \right], \quad (1)$$

where $J_i = \sum_{i=1}^N (\sigma_i/2)$ (σ are the Pauli matrices) describe N identical two-level systems of frequency Ω (often we will set $\Omega = 1$). The bosonic frequency is ω , and

$$\eta = \Omega N / \omega, \quad (2)$$

which plays a crucial role for the QPT. The physical coupling is $g = \tilde{g} \sqrt{\Omega \omega} / 2$, while λ controls the strength of counterrotating terms [32]. Note that $\eta \rightarrow \infty$ is realized by either $N \rightarrow \infty$ [31] or $\Omega/\omega \rightarrow \infty$ [1,2]. We initially assume $N = 1$, when $\lambda = 1$ is the QRM and $\lambda = 0$ is the JC model, and will treat later the case of general N .

Effective Hamiltonian.—To derive an effective theory, we note that the second term of Eq. (1) becomes dominant in the $\eta \rightarrow \infty$ limit of interest; thus, the relevant low-energy states have $\langle \sigma_x \rangle \simeq -1$. Within this subspace, the ground state is determined by the competition between the first term (a conventional oscillator) and the last term (the coupling between the bosonic mode and the two-level system). The coupling term has a larger prefactor, proportional to $\eta^{-1/2}$, but is off diagonal in σ_x . Thus, we partition H into the exactly solvable part H_0 (the first two terms) and the off-diagonal coupling V_{OD} . The second-order perturbation theory gives

$$H_{\text{eff}} \simeq \frac{p^2 + x^2}{2\eta} - \tilde{g}^2 \frac{(1+\lambda)^2 x^2 + (1-\lambda)^2 p^2}{8\eta} + \dots, \quad (3)$$

showing that the oscillator term is dominant in the normal phase (i.e., at weak coupling). On the other hand, at sufficiently large \tilde{g} the coupling term will dominate, and the Hamiltonian in Eq. (3) becomes unbounded. To this order of approximation, H_{eff} implies divergent values of $\langle x^2 \rangle$ and $\langle p^2 \rangle$, which in turn signals the onset of a superradiant phase at $\tilde{g}_c = 2/(1 + |\lambda|)$. This phase boundary is plotted in Fig. 1(a) as a solid (blue) line. The onset of instability in Eq. (3) is due to the x^2 (p^2) terms when $\lambda > 0$ ($\lambda < 0$), indicating the presence of an x -type (p -type) superradiant phase. This observation is reflected by the vertical (red) phase boundary in Fig. 1(a). The gap at $\xi < 1$ is also easily derived, and we plot it in Fig. 1(b).

Equation (3) recovers several important features of the QPT but can also be extended to a nonperturbative form. To higher orders, a generic contribution is given by a product of $2n$ matrix elements of V_{OD} (odd orders are zero) divided by $2n - 1$ energy denominators, which we take all equal to -1 in the limit of large η . After this approximation, the series becomes essentially identical to the perturbative treatment of the ground-state energy of $\sigma_z/2 + \epsilon \sigma_x$ [35].

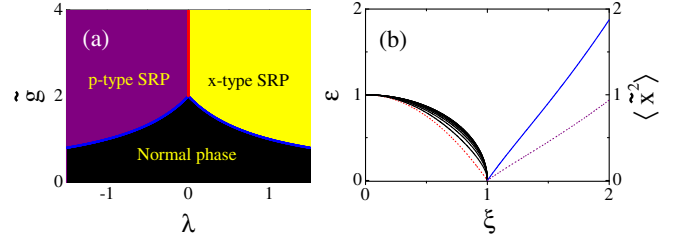


FIG. 1. (a) Phase diagram, where the blue (red) line indicates a second-order (first-order) QPT. (b) Energy gap of the normal phase ($\xi < 1$) at $\lambda = 0, 0.1, 0.2, \dots, 1$ (bottom to top), in units of $N\Omega/\eta$. The corresponding critical exponents are $\alpha = 1/2$ ($\lambda \neq 0$) and $\alpha = 1$ ($\lambda = 0$). For $\xi > 1$, we plot the order parameter $x_{0,\pm}^2$ at $\lambda \neq 0$ (solid curve) and $\lambda = 0$ (dotted curve, which is $1/2$ of the former). Panels (a) and (b) are both valid for arbitrary N .

The only difference is that $\langle V_{\text{OD}}^2 \rangle$ appears instead of ϵ^2 . Obviously, the series for the two-level system gives $-\sqrt{1/4 + \epsilon^2}$, which leads to

$$H_{\text{eff}} \simeq \frac{p^2 + x^2}{2\eta} - \sqrt{\frac{1}{4} + \frac{\xi^2 x^2 + \xi'^2 p^2 - \xi \xi'}{2\eta}}, \quad (4)$$

where $\xi = \tilde{g}(1 + \lambda)/2$ and $\xi' = \tilde{g}(1 - \lambda)/2$. The main idea of the derivation, given above, should clarify that Eq. (4) is an exact resummation of the leading perturbative terms, while more details can be found in Ref. [35].

Mean-field potential and mass renormalization.—We now discuss the main consequences of Eq. (4), and, for definiteness, we assume $\lambda > 0$ (x -type phase). Then, we may initially neglect the p operator:

$$H_{\text{eff}} \rightarrow \tilde{E}_-(\tilde{x}) = \frac{1}{2}(\tilde{x}^2 - \sqrt{1 + 2\xi^2 \tilde{x}^2}), \quad (5)$$

where $\tilde{x} = x/\sqrt{\eta}$ is a classical coordinate and \tilde{E}_- has the standard behavior of the Landau potential across a continuous phase transition, with ξ playing the role of the inverse temperature: \tilde{E}_- has one minimum at $\tilde{x} = 0$ when $\xi < 1$ and two minima at $\tilde{x}_{0,\pm} = \pm \sqrt{(\xi^2 - \xi^{-2})/2}$ when $\xi > 1$. The ground-state energy $\tilde{E}_{\text{gs}} = -\frac{1}{2} - \frac{1}{4}(\xi^2 + \xi^{-2} - 2)\theta(\xi - 1)$, where $\theta(x)$ is the step function, is easily obtained from Eq. (5) and indicates a second-order QPT at the critical value $\xi_c = 1$, in agreement with Fig. 1(a). We also emphasize that, although the anisotropy parameter λ influences the critical coupling strength \tilde{g}_c as well as $\tilde{x}_{0,\pm}$ and \tilde{E}_{gs} , the functional dependence of these physical quantities becomes universal—in the sense of being independent of λ —once it is formulated in terms of the rescaled coupling ξ . The order parameter $x_{0,\pm}^2$ is shown in Fig. 1(b).

To address the stability of the mean-field solution with respect to quantum fluctuations, we consider ($\tilde{p} = \eta p$):

$$H_{\text{eff}} \simeq \frac{\tilde{p}^2}{2M(\xi, \lambda)} + \tilde{E}_-(\tilde{x}), \quad (6)$$

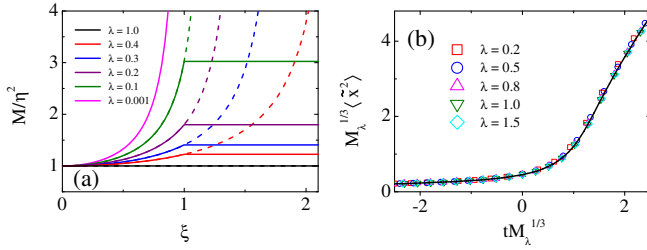


FIG. 2. (a) Effective mass renormalization as a function of ξ . For $\xi < 1$, $M = \eta^2(1 - \xi')^{-1}$, which in the absence of the superradiant phase would diverge at $\xi = (1 + \lambda)/(1 - \lambda)$ (dashed curves). Instead, $M = M_\lambda$ for $\xi > 1$. (b) Universal scaling function for $\langle \tilde{x}^2 \rangle$. Symbols are obtained by a solution of the full anisotropic QRM, with $\eta = 2^{20}$ and different values of λ . All numerical data collapse into the single function $X_1(v)$ (solid curve), obtained from Eq. (9).

where the kinetic term is obtained by expanding Eq. (4) in powers of p^2 and using $\tilde{x}^2 \approx \tilde{x}_{0,\pm}^2$. This yields

$$M(\xi, \lambda) = \eta^2 \left(1 - \xi'^2 / \sqrt{1 + 2\xi'^2 \tilde{x}_{0,\pm}^2} \right)^{-1} = \begin{cases} \eta^2(1 - \xi'^2)^{-1} & \text{for } \xi < 1 \\ \eta^2 \frac{(1+\lambda)^2}{4\lambda} \equiv M_\lambda & \text{for } \xi \geq 1, \end{cases} \quad (7)$$

which is an effective mass renormalized by the interaction, usually larger than the bare value $M(0, \lambda) = \eta^2$.

While fluctuations of p are generally promoted by the interaction, and in the normal phase Eq. (7) is in agreement with Eq. (3), an interesting competition exists in the broken-symmetry phase: The direct enhancement, which in the first line of Eq. (7) is due to the ξ'^2 factor, is partially compensated by a backaction through the order parameter, since a larger interaction also enhances the $\sqrt{1 + 2\xi'^2 \tilde{x}_{0,\pm}^2}$ denominator. The final result is a remarkable cancellation of the two effects, leading to an effective mass M_λ which is independent of ξ (or \tilde{g}).

Note that for $\xi > 1$ the effect of interaction is still present ($M_\lambda > \eta^2$) but only reflects anisotropy. As shown in Fig. 2(a) as a function of the interaction strength, the x -type superradiant order parameter acts as a background, freezing the effective mass at the $\xi = 1$ value. Furthermore, $M(\xi, \lambda = 1) = \eta^2$; i.e., the isotropic case has no mass renormalization. Therefore, the special interplay between the two quadratures of superradiance and the effective mass is specifically related to intermediate λ .

Finite- η scaling.—We can now derive a universal form of the critical scaling. At $\xi \approx 1$, the expressions of M_λ and \tilde{E}_- lead to

$$\tilde{H}_{\text{eff}} \approx \frac{\tilde{p}^2}{2M_\lambda} - \frac{1}{2} + \frac{\xi\xi'}{2\eta} + \frac{1 - \xi'^2}{2} \tilde{x}^2 + \frac{\xi^4}{4\eta} \tilde{x}^4, \quad (8)$$

where the potential is the small- \tilde{x} expansion of \tilde{E}_- , valid for $\langle \tilde{x}^2 \rangle \ll \eta|1 - \xi|$ [39]. Although the ground state ϕ_0 of

Eq. (8) depends in general on t , x , η , and λ (where $t = \xi - 1$), it actually satisfies

$$\left(-\frac{1}{2} \frac{\partial^2}{\partial u^2} - vu^2 + \frac{u^4}{4} \right) \phi_0(u, v) = E_0(v) \phi_0(u, v), \quad (9)$$

which is obtained by expressing Eq. (8) in terms of the scaling variables $u = \tilde{x}M_\lambda^{1/6}$ and $v = tM_\lambda^{1/3}$. $E_0(v)$ gives the ground-state energy of Eq. (8) through the following formula: $E_G(\lambda) \approx -\frac{1}{2} + (1/2\eta)[(1-\lambda)/(1+\lambda)] + M_\lambda^{-2/3} E_0(tM_\lambda^{1/3})$.

This treatment reveals the crucial role of M_λ in establishing the universal scaling laws of different observables, which are easily derived from the general form of the wave function $\phi_0(\tilde{x}M_\lambda^{1/6}, tM_\lambda^{1/3})$. For example, we find

$$\langle x^{2n} \rangle = \frac{\eta^n X_n(tM_\lambda^{1/3})}{M_\lambda^{n/3}}, \quad \langle p^{2n} \rangle = \frac{M_\lambda^{n/3} P_n(tM_\lambda^{1/3})}{\eta^n}, \quad (10)$$

where the universal functions $X_n(v)$ and $P_n(v)$ are simply the expectation values of u^n and $[-i(\partial/\partial u)]^n$ over $\phi_0(u, v)$ [35]. The validity of our treatment is confirmed by Figs. 2(b) and 3(a), showing that the numerical values of $\langle x^2 \rangle$ and $\langle p^2 \rangle$ at large η and different values of λ (obtained by the direct numerical diagonalization of the full Hamiltonian H [12,35,40]) all collapse into a single curve when appropriately scaled. The two numerical scaling functions agree with the $X_1(v)$ and $P_1(v)$ obtained from Eq. (9). Thus, the treatment provides an exact approach for the whole critical regime and is independent of λ . We have also performed a comparison to the variational scaling analysis at $\lambda = \xi = 1$ [2], which yields the exact critical exponents and an approximate prefactor, close to our exact result [35].

We finally conclude that the presence of anisotropy does not modify either the critical exponents or the scaling behavior and identify the whole second-order phase transition line as belonging to the same universality class [41]. Furthermore, as we discuss next, this universality can be extended to Eq. (1) with arbitrary N .

General N .—Although the procedure leading to Eq. (4) does not apply when $N > 1$, we can follow an alternative derivation of the mean-field potential \tilde{E}_- and effective mass M_λ , which we have identified as the crucial physical quantities. As before, we specialize the treatment to $\lambda > 0$, but the case $\lambda < 0$ can be treated in a similar way or by using the following mapping: $\mathcal{F} = \mathcal{F}_1 \otimes \mathcal{F}_2$, which contains a Z_2 symmetric mapping $\mathcal{F}_1: \{H(\lambda) \rightarrow H(-\lambda)\}$ and a unitary transformation $\mathcal{F}_2: \{H \rightarrow V^\dagger H V\}$, where $V = e^{-i(\pi/2)a^\dagger a} \otimes e^{-i(\pi/2)J_x}$. For any N , \mathcal{F} leaves the Hamiltonian invariant. Therefore, all the properties we discuss are readily translated to $\lambda < 0$.

\tilde{E}_- can be derived by applying to H the unitary transformation $U = e^{iJ_y \arctan \tilde{g}(1+\lambda)x/\sqrt{2\eta}}$, which gives

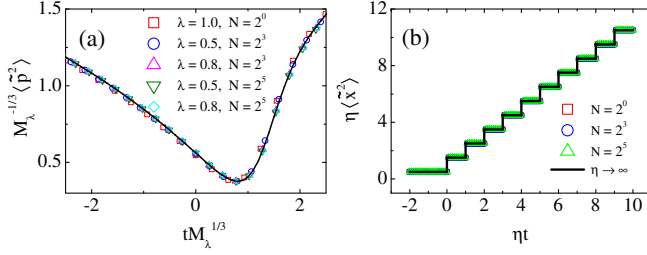


FIG. 3. Universal scaling functions at different values of λ and N . (a) Data collapse of numerical results, directly computed from H or the anisotropic Dicke model ($N > 1$). The solid curve is $P_1(v)$, obtained from Eq. (9). (b) Scaling function for $\langle x^2 \rangle = \langle p^2 \rangle$ at $\lambda = 0$. The numerical values (symbols) are in agreement with Eq. (13) (solid line).

$$U^\dagger \frac{H}{N} U \simeq \frac{x^2}{2\eta} + \frac{J_x}{N} \sqrt{1 + 2\xi^2 \frac{x^2}{\eta}} + \frac{p^2}{2\eta} + \sqrt{\frac{2}{\eta}} \frac{\xi^{\xi'} p}{\eta} \frac{J_y}{N}. \quad (11)$$

Using $\langle J_x \rangle \simeq -N/2$, we find that \tilde{E}_- (given by the first two terms) is the same of $N = 1$; thus, the phase diagram and order parameter are also unchanged (see Fig. 1).

While U was designed to diagonalize the coordinate dependence in H , we should now deal with the kinetic term. In Eq. (11), we have already performed an approximation, by neglecting the unitary transformation of the last two terms. This can be justified as follows: When $\eta \rightarrow \infty$, the problem approaches the classical limit; i.e., $x \simeq \sqrt{\eta} \tilde{x}_{0,\pm}$ has a well-defined value. Under this assumption, U commutes with the last two terms. Thus, Eq. (11) is correct to leading order in η .

Based on Eq. (11), we can apply the second-order perturbation theory and eliminate the off-diagonal J_y in the same way of Eq. (3). However, in Eq. (11), the energy gap is nonperturbatively enhanced by the superradiant phase. It is equal to $1/N \sqrt{1 + 2\xi^2 \tilde{x}_{0,\pm}^2}$ to leading order in η , which gives the same effective mass we have discussed for $N = 1$ (see Fig. 2). This alternative derivation gives a concrete physical meaning to the denominator leading to Eq. (7); i.e., it is a renormalized energy gap.

We can finally conclude that all these models have not only the same phase diagram but also the same critical behavior. This is because the finite- η scaling properties are fully determined by \tilde{E}_- and M_λ ; thus, they must be independent of N and λ . In Fig. 3(a), we verify that the numerical scaling functions are indeed identical and coincide with the universal result obtained from the effective Hamiltonian [Eqs. (8) and (9)].

The JC critical line.—The $\lambda = 0$ line is excluded by the behavior we have discussed so far. For $\xi > 1$, it defines a first-order transition line [27,31] where the order parameters and scaling functions have an abrupt change. Since the exact mapping between opposite values of λ interchanges the roles of x and p , the two right-hand sides of Eq. (10)

must be switched when $\lambda < 0$ (together with the changes $M_\lambda \rightarrow M_{-\lambda}$ and $t \rightarrow \xi' - 1$). This argument, however, does not give any information on the scaling functions at $\lambda = 0$.

To address this question, we have computed the corrections to the energy of the unperturbed ($g = 0$) eigenstates $|q\rangle \otimes |-N/2\rangle$, where $|q\rangle = |0\rangle, |1\rangle, \dots$ are Fock states:

$$\frac{E_{\text{JC}}(q)}{N} = -\frac{1}{2} + \frac{q}{\eta} + \frac{\xi^2 q}{\eta - N} + \frac{\xi^4}{\eta^2} q(q + N - 1). \quad (12)$$

This expression includes all the $O(\eta^{-2})$ terms and allows us to find the energy level crossing points ξ_q with $O(\eta^{-1})$ accuracy. Although Eq. (12) has an explicit dependence on N , this disappears by solving $E_{\text{JC}}(q) = E_{\text{JC}}(q + 1)$, which gives $\xi_q = 1 + q/\eta + O(\eta^{-2})$. Thus, the level crossings have an equal spacing of $1/\eta$. It is also easy to check that in the $\eta \rightarrow \infty$ limit the admixture of $|q\rangle \otimes |-N/2\rangle$ with other states is negligible. These considerations imply again that the scaling functions are independent of N . Equation (10) is replaced by

$$\langle x^{2n} \rangle = \langle p^{2n} \rangle = 1 + \sum_{q=0}^{\infty} \theta\left(t - \frac{q}{\eta}\right) (\langle x^{2n} \rangle_{q+1} - \langle x^{2n} \rangle_q), \quad (13)$$

where $\langle x^{2n} \rangle_q = \langle q | x^{2n} | q \rangle = (2n - 1)!! D(n, q) / 2^n$ [here $D(n, q)$ are the Delannoy numbers [42]]. The case $n = 1$ is shown in Fig. 3(b) and should be compared to Figs. 2(b) and 3(a). We see that η plays the role of $M_\lambda^{1/3}$ (which is not defined at $\lambda = 0$). In particular, we have the very peculiar finding of discontinuous scaling functions, despite the fact that other features (e.g., the order parameter and gap) behave like in a regular phase transition. As is clear from our derivation, the scaling functions still reflect the fact that the QPT of the JC limit is given by a succession of level crossings. This is true for arbitrary N and highlights the singular nature of the $\lambda = 0$ line within the phase diagram. In particular, the scaling functions are nonanalytic: They depend on the order of the two limits $\lambda \rightarrow 0$ and $\eta \rightarrow \infty$.

Conclusion.—We have characterized the QPTs of the QRM as a function of the coupling strength and anisotropy and established the universal character of the second-order phase transition. Besides universality, we have found other interesting features such as the freezing of the effective mass (induced by the broken symmetry in x) and the discontinuous scaling functions of the JC model. Our results emphasize the critical role played by counterrotating terms, whose current experimental relevance is due to the rapid progress in enhancing light-matter interactions [3–16,43,44]. In particular, the exposed singularity of the JC limit implies that even tiny counterrotating terms lead to dramatic changes of the scaling behavior. We also note that the superradiant phase leads to a strongly squeezed ground

state of light, which has potential value for metrology and enhanced sensing applications.

All these findings are extended to $N > 1$, with the simple (but significant) consequence that the few-body QPT can be equivalently observed at a smaller coupling strength ($g_c \rightarrow g_c/\sqrt{N}$) and a larger ω/Ω (since $\eta \rightarrow N\eta$). A smaller g and larger ω should make the implementation easier and more resilient to environmental noise. From a more theoretical perspective, this class of physical models exhibits a stronger form of universality, since not only the critical exponents and scaling functions are independent on N and λ but also other nonuniversal features, e.g., the critical coupling and order parameter. Thus, scattered findings of identical behavior of the $N = 1$ and the more conventional $N \rightarrow \infty$ limit [1,2,26–28,31] are reconciled into a general framework. Although we have not explicitly discussed the critical dynamics [1,26,28], also in that case the scaling functions are expected to be identical at arbitrary N and λ . This is indeed true for the special case $\lambda = 0$ and the two extreme limits, $N = 1$ or $N \rightarrow \infty$ [26]. Another interesting question is how interactions among the two-level systems (see, e.g., Ref. [27]) would affect these conclusions.

This work is supported by National Science Foundation of China (Grants No. 11604009, No. 11574025, No. 11325417, No. 11674139, and No. 1121403) and National Scholastic Athletics Foundation (Grant No. U1530401). Z.-J.Y. acknowledges the Future and Emerging Technologies (FET) program under FET-Open Grant No. 618083 (Curved Nanomembranes for Topological Quantum Computation). We also acknowledge the computational support in Beijing Computational Science Research Center (CSRC).

*stefano.chesi@csrc.ac.cn

[†]Present address: CNR-SPIN and Dipartimento di Fisica “E. R. Caianiello”, Università di Salerno, I-84084 Fisciano, Italy.

[‡]luohg@lzu.edu.cn

- [1] M.-J. Hwang, R. Puebla, and M. B. Plenio, *Phys. Rev. Lett.* **115**, 180404 (2015).
- [2] M.-J. Hwang and M. B. Plenio, *Phys. Rev. Lett.* **117**, 123602 (2016).
- [3] A. Wallraff, D. I. Schuster, A. Blais, L. Frunzio, R.-S. Huang, J. Majer, S. Kumar, S. M. Girvin, and R. J. Schoelkopf, *Nature (London)* **431**, 162 (2004).
- [4] M. Devoret, S. Girvin, and R. Schoelkopf, *Ann. Phys. (Berlin)* **16**, 767 (2007).
- [5] J. Bourassa, J. M. Gambetta, A. A. Abdumalikov, O. Astafiev, Y. Nakamura, and A. Blais, *Phys. Rev. A* **80**, 032109 (2009).
- [6] T. Niemczyk, F. Deppe, H. Huebl, E. P. Menzel, F. Hocke, M. J. Schwarz, J. J. García-Ripoll, D. Zueco, T. Hümmer, E. Solano, A. Marx, and R. Gross, *Nat. Phys.* **6**, 772 (2010).
- [7] B. Peropadre, P. Forn-Díaz, E. Solano, and J. J. García-Ripoll, *Phys. Rev. Lett.* **105**, 023601 (2010).
- [8] A. Ridolfo, M. Leib, S. Savasta, and M. J. Hartmann, *Phys. Rev. Lett.* **109**, 193602 (2012).
- [9] Y. Todorov and C. Sirtori, *Phys. Rev. X* **4**, 041031 (2014).
- [10] A. Baust, E. Hoffmann, M. Haerberlein, M. J. Schwarz, P. Eder, J. Goetz, F. Wulschner, E. Xie, L. Zhong, F. Quijandría, D. Zueco, J.-J. García Ripoll, L. García-Álvarez, G. Romero, E. Solano, K. G. Fedorov, E. P. Menzel, F. Deppe, A. Marx, and R. Gross, *Phys. Rev. B* **93**, 214501 (2016).
- [11] P. Forn-Díaz, G. Romero, C. J. P. M. Harmans, E. Solano, and J. E. Mooij, *Sci. Rep.* **6**, 26720 (2016).
- [12] J. Casanova, G. Romero, I. Lizuain, J. J. García-Ripoll, and E. Solano, *Phys. Rev. Lett.* **105**, 263603 (2010).
- [13] S. De Liberato, *Phys. Rev. Lett.* **112**, 016401 (2014).
- [14] P. Forn-Díaz, J. J. García-Ripoll, B. Peropadre, J. L. Orgiazzi, M. A. Yurtalan, R. Belyansky, C. M. Wilson, and A. Lupascu, *Nat. Phys.* **13**, 39 (2017).
- [15] F. Yoshihara, T. Fuse, S. Ashhab, K. Kakuyanagi, S. Saito, and K. Semba, *Nat. Phys.* **13**, 44 (2017).
- [16] Z. Chen, Y. Wang, T. Li, L. Tian, Y. Qiu, K. Inomata, F. Yoshihara, S. Han, F. Nori, J. S. Tsai, and J. Q. You, *Phys. Rev. A* **96**, 012325 (2017).
- [17] P. Forn-Díaz, J. Lisenfeld, D. Marcos, J. J. García-Ripoll, E. Solano, C. J. P. M. Harmans, and J. E. Mooij, *Phys. Rev. Lett.* **105**, 237001 (2010).
- [18] D. Braak, *Phys. Rev. Lett.* **107**, 100401 (2011).
- [19] E. Solano, *Physics* **4**, 68 (2011).
- [20] L. Bakemeier, A. Alvermann, and H. Fehske, *Phys. Rev. A* **85**, 043821 (2012).
- [21] Q.-H. Chen, C. Wang, S. He, T. Liu, and K.-L. Wang, *Phys. Rev. A* **86**, 023822 (2012).
- [22] S. Ashhab, *Phys. Rev. A* **87**, 013826 (2013).
- [23] F. A. Wolf, F. Vallone, G. Romero, M. Kollar, E. Solano, and D. Braak, *Phys. Rev. A* **87**, 023835 (2013).
- [24] Z.-J. Ying, M. Liu, H.-G. Luo, H.-Q. Lin, and J. Q. You, *Phys. Rev. A* **92**, 053823 (2015).
- [25] D. Braak, Q.-H. Chen, M. T. Batchelor, and E. Solano, *J. Phys. A* **49**, 300301 (2016).
- [26] R. Puebla, M.-J. Hwang, J. Casanova, and M. B. Plenio, *Phys. Rev. Lett.* **118**, 073001 (2017).
- [27] W.-J. Yang and X.-B. Wang, *Phys. Rev. A* **95**, 043823 (2017).
- [28] L.-T. Shen, Z.-B. Yang, H.-Z. Wu, and S.-B. Zheng, *Phys. Rev. A* **95**, 013819 (2017).
- [29] J. Schliemann, J. C. Egues, and D. Loss, *Phys. Rev. B* **67**, 085302 (2003).
- [30] Z. H. Wang, Q. Zheng, X. Wang, and Y. Li, *Sci. Rep.* **6**, 22347 (2016).
- [31] A. Baksic and C. Ciuti, *Phys. Rev. Lett.* **112**, 173601 (2014).
- [32] Q.-T. Xie, S. Cui, J.-P. Cao, L. Amico, and H. Fan, *Phys. Rev. X* **4**, 021046 (2014).
- [33] R. Puebla, J. Casanova, and M. B. Plenio, *New J. Phys.* **18**, 113039 (2016).
- [34] J. M. Raimond, M. Brune, and S. Haroche, *Rev. Mod. Phys.* **73**, 565 (2001).
- [35] See Supplemental Material at <http://link.aps.org/supplemental/10.1103/PhysRevLett.119.220601> for the derivation of useful effective Hamiltonians, expectation values, and the scaling functions of the JC model, as well

- as further details on the numerical scaling analysis (including Refs. [36–38]).
- [36] F. L. Pedrocchi, S. Chesi, and D. Loss, *Phys. Rev. B* **83**, 115415 (2011).
- [37] R. Winkler, *Spin-Orbit Coupling Effects in Two-Dimensional Electron and Hole Systems* (Springer, Berlin, 2003).
- [38] M. Liu, Z.-J. Ying, J.-H. An, and H.-G. Luo, *New J. Phys.* **17**, 043001 (2015).
- [39] Since $\langle x^2 \rangle$ and $\langle p^2 \rangle$ are small in this regime, one can confirm Eq. (8) using the Schrieffer-Wolff transformation up to fourth order [35]. However, this misses the interesting nonperturbative physics discussed so far.
- [40] D. Braak, *J. Phys. A* **46**, 175301 (2013).
- [41] J. Larson and E. K. Irish, *J. Phys. A* **50**, 174002 (2017).
- [42] H. Delannoy, *Assoc. Franc. Bordeaux* **24**, 70 (1895).
- [43] S. Gröblacher, K. Hammerer, M. R. Vanner, and M. Aspelmeyer, *Nature (London)* **460**, 724 (2009).
- [44] G. Günter, A. A. Anappara, J. Hees, A. Sell, G. Biasiol, L. Sorba, S. De Liberato, C. Ciuti, A. Tredicucci, A. Leitenstorfer, and R. Huber, *Nature (London)* **458**, 178 (2009).